

World Journal of *Clinical Cases*

World J Clin Cases 2021 July 26; 9(21): 5754-6177



REVIEW

- 5754 Treatment strategies for hepatocellular carcinoma with extrahepatic metastasis
Long HY, Huang TY, Xie XY, Long JT, Liu BX

MINIREVIEWS

- 5769 Prevention of hepatitis B reactivation in patients requiring chemotherapy and immunosuppressive therapy
Shih CA, Chen WC
- 5782 Research status on immunotherapy trials of gastric cancer
Liang C, Wu HM, Yu WM, Chen W
- 5794 Therapeutic plasma exchange for hyperlipidemic pancreatitis: Current evidence and unmet needs
Zheng CB, Zheng ZH, Zheng YP
- 5804 Essentials of thoracic outlet syndrome: A narrative review
Chang MC, Kim DH

ORIGINAL ARTICLE**Case Control Study**

- 5812 Soluble programmed death-1 is predictive of hepatitis B surface antigen loss in chronic hepatitis B patients after antiviral treatment
Tan N, Luo H, Kang Q, Pan JL, Cheng R, Xi HL, Chen HY, Han YF, Yang YP, Xu XY

Retrospective Cohort Study

- 5822 Tunneled biopsy is an underutilised, simple, safe and efficient method for tissue acquisition from subepithelial tumours
Koutsoumpas A, Perera R, Melton A, Kuker J, Ghosh T, Braden B

Retrospective Study

- 5830 Macular ganglion cell complex injury in different stages of anterior ischemic optic neuropathy
Zhang W, Sun XQ, Peng XY
- 5840 Value of refined care in patients with acute exacerbation of chronic obstructive pulmonary disease
Na N, Guo SL, Zhang YY, Ye M, Zhang N, Wu GX, Ma LW
- 5850 Facilitators and barriers to colorectal cancer screening in an outpatient setting
Samuel G, Kratzer M, Asagbra O, Kinderwater J, Poola S, Udom J, Lambert K, Mian M, Ali E
- 5860 Development and validation of a prognostic nomogram for colorectal cancer after surgery
Li BW, Ma XY, Lai S, Sun X, Sun MJ, Chang B

Observational Study

- 5873 Potential protein-phenotype correlation in three lipopolysaccharide-responsive beige-like anchor protein-deficient patients

Tang WJ, Hu WH, Huang Y, Wu BB, Peng XM, Zhai XW, Qian XW, Ye ZQ, Xia HJ, Wu J, Shi JR

- 5889 Quantification analysis of pleural line movement for the diagnosis of pneumothorax

Xiao R, Shao Q, Zhao N, Liu F, Qian KJ

Prospective Study

- 5900 Preprocedure ultrasound imaging combined with palpation technique in epidural labor analgesia

Wu JP, Tang YZ, He LL, Zhao WX, An JX, Ni JX

Randomized Controlled Trial

- 5909 Effects of perioperative rosuvastatin on postoperative delirium in elderly patients: A randomized, double-blind, and placebo-controlled trial

Xu XQ, Luo JZ, Li XY, Tang HQ, Lu WH

SYSTEMATIC REVIEWS

- 5921 Pain assessment and management in the newborn: A systematized review

Garcia-Rodriguez MT, Bujan-Bravo S, Seijo-Bestilleiro R, Gonzalez-Martin C

META-ANALYSIS

- 5932 Fatigue prevalence in men treated for prostate cancer: A systematic review and meta-analysis

Luo YH, Yang YW, Wu CF, Wang C, Li WJ, Zhang HC

CASE REPORT

- 5943 Diagnostic discrepancy between colposcopy and vaginoscopy: A case report

Li Q, Zhang HW, Sui L, Hua KQ

- 5948 Contrast enhanced ultrasound in diagnosing liver lesion that spontaneously disappeared: A case report

Wang ZD, Haitham S, Gong JP, Pen ZL

- 5955 COVID-19 patient with an incubation period of 27 d: A case report

Du X, Gao Y, Kang K, Chong Y, Zhang ML, Yang W, Wang CS, Meng XL, Fei DS, Dai QQ, Zhao MY

- 5963 Awake extracorporeal membrane oxygenation support for a critically ill COVID-19 patient: A case report

Zhang JC, Li T

- 5972 Meigs syndrome with pleural effusion as initial manifestation: A case report

Hou YY, Peng L, Zhou M

- 5980 Giant hemangioma of the caudate lobe of the liver with surgical treatment: A case report

Wang XX, Dong BL, Wu B, Chen SY, He Y, Yang XJ

- 5988** Anti-programmed cell death ligand 1-based immunotherapy in recurrent hepatocellular carcinoma with inferior vena cava tumor thrombus and metastasis: Three case reports
Liu SR, Yan Q, Lin HM, Shi GZ, Cao Y, Zeng H, Liu C, Zhang R
- 5999** Minimal deviation adenocarcinoma with elevated CA19-9: A case report
Dong Y, Lv Y, Guo J, Sun L
- 6005** Isolated fungus ball in a single cell of the left ethmoid roof: A case report
Zhou LQ, Li M, Li YQ, Wang YJ
- 6009** Rare case of brucellosis misdiagnosed as prostate carcinoma with lumbar vertebra metastasis: A case report
Yan JF, Zhou HY, Luo SF, Wang X, Yu JD
- 6017** Myeloid sarcoma of the colon as initial presentation in acute promyelocytic leukemia: A case report and review of the literature
Wang L, Cai DL, Lin N
- 6026** Primary follicular lymphoma in the renal pelvis: A rare case report
Shen XZ, Lin C, Liu F
- 6032** Rosai-Dorfman disease in the spleen of a pediatric patient: A case report
Ryu H, Hwang JY, Kim YW, Kim TU, Jang JY, Park SE, Yang EJ, Shin DH
- 6041** Relapsed/refractory classical Hodgkin lymphoma effectively treated with low-dose decitabine plus tislelizumab: A case report
Ding XS, Mi L, Song YQ, Liu WP, Yu H, Lin NJ, Zhu J
- 6049** Disseminated *Fusarium* bloodstream infection in a child with acute myeloid leukemia: A case report
Ning JJ, Li XM, Li SQ
- 6056** Familial hemophagocytic lymphohistiocytosis type 2 in a female Chinese neonate: A case report and review of the literature
Bi SH, Jiang LL, Dai LY, Wang LL, Liu GH, Teng RJ
- 6067** Usefulness of metagenomic next-generation sequencing in adenovirus 7-induced acute respiratory distress syndrome: A case report
Zhang XJ, Zheng JY, Li X, Liang YJ, Zhang ZD
- 6073** Neurogenic orthostatic hypotension with Parkinson's disease as a cause of syncope: A case report
Li Y, Wang M, Liu XL, Ren YF, Zhang WB
- 6081** SATB2-associated syndrome caused by a novel SATB2 mutation in a Chinese boy: A case report and literature review
Zhu YY, Sun GL, Yang ZL
- 6091** Diagnosis and treatment discussion of congenital factor VII deficiency in pregnancy: A case report
Yang Y, Zeng YC, Rumende P, Wang CG, Chen Y

- 6102** Unusual immunohistochemical “null” pattern of four mismatch repair proteins in gastric cancer: A case report
Yue M, Liu JY, Liu YP
- 6110** Generalized periodontitis treated with periodontal, orthodontic, and prosthodontic therapy: A case report
Kaku M, Matsuda S, Kubo T, Shimoe S, Tsuga K, Kurihara H, Tanimoto K
- 6125** Ligamentum flavum hematoma following a traffic accident: A case report
Yu D, Lee W, Chang MC
- 6130** Oral cyclophosphamide-induced posterior reversible encephalopathy syndrome in a patient with ANCA-associated vasculitis: A case report
Kim Y, Kwak J, Jung S, Lee S, Jang HN, Cho HS, Chang SH, Kim HJ
- 6138** Encapsulating peritoneal sclerosis in an AMA-M2 positive patient: A case report
Yin MY, Qian LJ, Xi LT, Yu YX, Shi YQ, Liu L, Xu CF
- 6145** Multidisciplinary diagnostic dilemma in differentiating Madelung’s disease – the value of superb microvascular imaging technique: A case report
Seskute G, Dapkute A, Kausaite D, Strainiene S, Talijunas A, Butrimiene I
- 6155** Complicated course of biliary inflammatory myofibroblastic tumor mimicking hilar cholangiocarcinoma: A case report and literature review
Strainiene S, Sedleckaite K, Jarasunas J, Savlan I, Stanaitis J, Stundiene I, Strainys T, Liakina V, Valantinas J
- 6170** Fruquintinib beneficial in elderly patient with neoplastic pericardial effusion from rectal cancer: A case report
Zhang Y, Zou JY, Xu YY, He JN

ABOUT COVER

Editorial Board Member of *World Journal of Clinical Cases*, Jae Gil Lee, MD, PhD, Professor, Surgeon, Department of Surgery, Yonsei University College of Medicine, Seoul 03722, South Korea. jakii@yuhs.ac

AIMS AND SCOPE

The primary aim of *World Journal of Clinical Cases* (*WJCC*, *World J Clin Cases*) is to provide scholars and readers from various fields of clinical medicine with a platform to publish high-quality clinical research articles and communicate their research findings online.

WJCC mainly publishes articles reporting research results and findings obtained in the field of clinical medicine and covering a wide range of topics, including case control studies, retrospective cohort studies, retrospective studies, clinical trials studies, observational studies, prospective studies, randomized controlled trials, randomized clinical trials, systematic reviews, meta-analysis, and case reports.

INDEXING/ABSTRACTING

The *WJCC* is now indexed in Science Citation Index Expanded (also known as SciSearch®), Journal Citation Reports/Science Edition, Scopus, PubMed, and PubMed Central. The 2021 Edition of Journal Citation Reports® cites the 2020 impact factor (IF) for *WJCC* as 1.337; IF without journal self cites: 1.301; 5-year IF: 1.742; Journal Citation Indicator: 0.33; Ranking: 119 among 169 journals in medicine, general and internal; and Quartile category: Q3. The *WJCC*'s CiteScore for 2020 is 0.8 and Scopus CiteScore rank 2020: General Medicine is 493/793.

RESPONSIBLE EDITORS FOR THIS ISSUE

Production Editor: *Ji-Hong Lin*; Production Department Director: *Xiang Li*; Editorial Office Director: *Jim-Lai Wang*.

NAME OF JOURNAL

World Journal of Clinical Cases

ISSN

ISSN 2307-8960 (online)

LAUNCH DATE

April 16, 2013

FREQUENCY

Thrice Monthly

EDITORS-IN-CHIEF

Dennis A Bloomfield, Sandro Vento, Bao-Gan Peng

EDITORIAL BOARD MEMBERS

<https://www.wjgnet.com/2307-8960/editorialboard.htm>

PUBLICATION DATE

July 26, 2021

COPYRIGHT

© 2021 Baishideng Publishing Group Inc

INSTRUCTIONS TO AUTHORS

<https://www.wjgnet.com/bpg/gerinfo/204>

GUIDELINES FOR ETHICS DOCUMENTS

<https://www.wjgnet.com/bpg/GerInfo/287>

GUIDELINES FOR NON-NATIVE SPEAKERS OF ENGLISH

<https://www.wjgnet.com/bpg/gerinfo/240>

PUBLICATION ETHICS

<https://www.wjgnet.com/bpg/GerInfo/288>

PUBLICATION MISCONDUCT

<https://www.wjgnet.com/bpg/gerinfo/208>

ARTICLE PROCESSING CHARGE

<https://www.wjgnet.com/bpg/gerinfo/242>

STEPS FOR SUBMITTING MANUSCRIPTS

<https://www.wjgnet.com/bpg/GerInfo/239>

ONLINE SUBMISSION

<https://www.f6publishing.com>

Observational Study

Quantification analysis of pleural line movement for the diagnosis of pneumothorax

Rui Xiao, Qiang Shao, Ning Zhao, Fen Liu, Ke-Jian Qian

ORCID number: Rui Xiao 0000-0002-9070-4970; Qiang Shao 0000-0002-4136-7680; Ning Zhao 0000-0002-1683-0039; Fen Liu 0000-0003-4431-3394; Ke-Jian Qian 0000-0002-9074-0409.

Author contributions: Xiao R and Qian KJ were the guarantors and designed the study; Xiao R and Zhao N participated in the acquisition, analysis, and interpretation of the data, and drafted the initial manuscript; Shao Q and Liu F revised the manuscript.

Institutional review board

statement: This study was approved by the Ethics Committee of the First Affiliated Hospital of Nanchang University.

Informed consent statement:

Written consent was obtained from all subjects.

Conflict-of-interest statement: The

authors have no conflicts of interest to disclose.

Data sharing statement: The datasets used and/or analyzed during the current study are available from the corresponding author on reasonable request.

STROBE statement: The authors have read the STROBE Statement,

Rui Xiao, Qiang Shao, Ning Zhao, Fen Liu, Ke-Jian Qian, Department of Intensive Care Medicine, First Affiliated Hospital of Nanchang University, Nanchang 330006, Jiangxi Province, China

Corresponding author: Ke-Jian Qian, MD, PhD, Full Professor, Department of Intensive Care Medicine, First Affiliated Hospital of Nanchang University, No. 17 Yongwaizheng Road, Nanchang 330006, Jiangxi Province, China. ndyfyicu@email.ncu.edu.cn

Abstract**BACKGROUND**

There is no research on quantitative pleural line movement. In this study, we assume that tissue Doppler and its quantitative technology can quantify the pleural line movement and can be used to diagnose pneumothorax.

AIM

To evaluate the quantitative assessment of pleural line movement measured by tissue Doppler imaging (TDI) for pneumothorax diagnosis.

METHODS

Adult patients ($n = 45$) diagnosed with unilateral pneumothorax were included in this study. Each patient underwent TDI of both lungs. The pneumothorax side and contralateral normal lung side were compared using several indices obtained from TDI: peak pleural line velocity (PV_{max}), peak chest wall tissue velocity (CV_{max}), peak pleural line strain value (PS_{max}), peak chest wall tissue strain value (CS_{max}), PV_{max}/CV_{max} and PS_{max}/CS_{max}. The receiver operating characteristic analysis was used to evaluate the performance of these quantitative assessments for pneumothorax diagnosis.

RESULTS

Various quantitative variables of the pneumothorax side were all lower than that of the non-pneumothorax side and included the PV_{max} (0.36 cm/s vs 0.59 cm/s, $P < 0.001$), PS_{max} (1.14% vs 1.90%, $P = 0.001$), PV_{max}/CV_{max} (1.06 vs 4.93, $P < 0.001$), and PS_{max}/CS_{max} (0.76 vs 1.74, $P < 0.001$). For the discrimination of pneumothorax, the cut-off values of the PV_{max}, PS_{max}, PV_{max}/CV_{max} and PS_{max}/CS_{max} were calculated as 0.50 cm/s, 0.94%, 1.96, and 1.12, respectively. Similarly, the sensitivities and specificities of PV_{max}, PS_{max}, PV_{max}/CV_{max} and PS_{max}/CS_{max} were 96% and 62%, 47% and 91%, 93% and 96%, and 82% and 93%, respectively. The area under the receiver operating characteristic curve were 0.84, 0.72, 0.99, and 0.91, respectively, for PV_{max}, PS_{max}, PV_{max}/CV_{max} and PS_{max}/CS_{max}.

and the manuscript was prepared and revised according to the STROBE Statement.

Open-Access: This article is an open-access article that was selected by an in-house editor and fully peer-reviewed by external reviewers. It is distributed in accordance with the Creative Commons Attribution NonCommercial (CC BY-NC 4.0) license, which permits others to distribute, remix, adapt, build upon this work non-commercially, and license their derivative works on different terms, provided the original work is properly cited and the use is non-commercial. See: <http://creativecommons.org/licenses/by-nc/4.0/>

Manuscript source: Unsolicited manuscript

Specialty type: Medicine, research and experimental

Country/Territory of origin: China

Peer-review report's scientific quality classification

Grade A (Excellent): 0
Grade B (Very good): 0
Grade C (Good): C
Grade D (Fair): 0
Grade E (Poor): 0

Received: February 19, 2021

Peer-review started: February 19, 2021

First decision: March 11, 2021

Revised: March 19, 2021

Accepted: June 1, 2021

Article in press: June 1, 2021

Published online: July 26, 2021

P-Reviewer: Vetrugno L

S-Editor: Fan JR

L-Editor: Filipodia

P-Editor: Xing YX



CONCLUSION

Quantification analysis of pleural line movement using TDI is a useful tool for the diagnosis of pneumothorax.

Key Words: Lung ultrasound; Pneumothorax; Tissue Doppler imaging; Pleural line movement

©The Author(s) 2021. Published by Baishideng Publishing Group Inc. All rights reserved.

Core Tip: This study used tissue Doppler to quantify the movement of the pleural line for the diagnosis of pneumothorax in patients with unilateral pneumothorax. Various quantitative variables of the pneumothorax side were all lower than that of the non-pneumothorax side. Peak pleural line velocity/peak chest wall tissue velocity was the best variable to diagnose pneumothorax (area under receiver operating characteristic curve, 0.99). Tissue Doppler quantitative technique is an effective tool for the diagnosis of pneumothorax.

Citation: Xiao R, Shao Q, Zhao N, Liu F, Qian KJ. Quantification analysis of pleural line movement for the diagnosis of pneumothorax. *World J Clin Cases* 2021; 9(21): 5889-5899

URL: <https://www.wjgnet.com/2307-8960/full/v9/i21/5889.htm>

DOI: <https://dx.doi.org/10.12998/wjcc.v9.i21.5889>

INTRODUCTION

Pneumothorax is characterized by sudden dyspnea, respiratory distress, chest pain, cough, or decreased blood oxygen saturation and is a common and critical acute condition. A timely diagnosis can improve patient outcomes. However, in practice pneumothorax diagnosis requires further discrimination with other conditions. Pneumothorax is easily diagnosed using radiological tools, such as chest radiograph and computed tomography (CT)[1]. For pneumothorax diagnosis, CT has several disadvantages, such as radiation exposure, cost, and availability[2]. Although chest radiograph is more convenient than CT, its sensitivity in the diagnosis of pneumothorax is relatively low and is estimated to be only around 20.9%[3].

Due to its easy access, ultrasound has been widely used in emergency departments and intensive care units. Recently, lung ultrasound has been evaluated for the diagnosis of pneumothorax. For example, among intensive care unit patients, lung ultrasound was found to be a useful tool for pneumothorax diagnosis with a sensitivity of 75% and a specificity of 93%[4]. Currently, the criteria of ultrasound diagnosis for pneumothorax are as follows: absence of lung sliding[5], lung point[6,7], and barcode sign[6]. Of these, the absence of lung sliding is the most common sign for pneumothorax diagnosis and has been listed in the bedside lung ultrasound in emergency protocol[8]. Unfortunately, pneumothorax diagnosis using lung ultrasound still faces several challenges. First, the ultrasonic features of pneumothorax are similar to a wide range of other diseases that include severe asthma[9], pulmonary bullae[10], and chronic obstructive pulmonary disease[11]. Second, the ultrasonic method for pneumothorax diagnosis depends on the physician's experience and training[12]. Third, the movement of the pleural line is based on the movement of the visceral and parietal pleura during respiration, and the evaluation of movement using ultrasound is subjective and may vary between observers. In addition, patient postures may also have a significant impact on the diagnosis[13].

Usually, tissue Doppler imaging (TDI) is performed to quantitatively evaluate cardiac function, including systolic and diastolic cycles[14,15]. Moreover, it is also advised to evaluate the synchronization of left ventricular myocardial contraction by tissue velocity imaging and strain quantitative technology[16]. Recently, we found that TDI can quantify the movement of the pleural line. Therefore, in this prospective study, we aimed to evaluate the performance of TDI for pneumothorax diagnosis by quantitative analysis of pleural line movement during respiration.

MATERIALS AND METHODS

Ethics

This study was approved by the Ethics Committee of the First Affiliated Hospital of Nanchang University, and written consent was obtained from all subjects. This study was performed in accordance with the Declaration of Helsinki (2013).

Patients

Between September 2019 and May 2020, adult patients (> 18 years) who were admitted to the emergency department and intensive care unit at our center with unilateral pneumothorax confirmed by CT were included for further analysis. Lung ultrasound was performed 2 h after CT examination. Patients were excluded if they presented with bilateral pneumothorax, if cardiac monitoring was absent from ultrasound images, or if invasive mechanical ventilation was performed. Patient characteristics such as age, sex, weight, height, etiology, and pneumothorax side were collected for further analysis.

Lung ultrasound

Ultrasound examination was performed by a senior physician with > 5 years of experience in lung ultrasonography. The examination was performed with a Mindray Ultrasound Scanning machine (M8/M9, Mindray, Shenzhen, China) equipped with low frequency transducers (1-5 MHz and 2-4 MHz). Ultrasonic images were analyzed with the TDI-QA software (Mindray, Shenzhen, China). Lung ultrasound was performed for patients with pneumothorax by a specific investigator (RX). Briefly, the ultrasound was performed as follows. First, the patient laid in the supine position, and the probe was positioned perpendicularly to the chest wall. For the pneumothorax side, if the pleural line movement disappeared, tissue Doppler was switched, and ultrasonic images were collected for at least 20 s. For the non-pneumothorax side, ultrasound images were collected at the contralateral site.

Ultrasonographic data were selected retrospectively. Quantitative analysis of ultrasonic images was performed as shown in Figures 1 and 2. Briefly, the diameter of the region of interest (ROI) was adjusted to the width of the pleural line, and then the first ROI (ROI1, red) was placed at the midpoint of the pleural line. Subsequently, a velocity-time curve and a strain-time curve were generated automatically. Meanwhile, the maximum velocity and strain were calculated based on the quantitative analysis and included the peak pleural line velocity (PV_{max}) and peak pleural line strain value (PS_{max}). The second ROI (ROI2, yellow) was placed in the chest wall tissue about 0.5 cm from ROI1. The software automatically generated a velocity-time curve and a strain-time curve, measuring the maximum chest wall tissue velocity and maximum strain. These parameters are called peak chest wall tissue velocity (CV_{max}) and peak chest wall tissue strain value (CS_{max}). All above-mentioned indexes, including the PV_{max}/CV_{max} and PS_{max}/CS_{max} ratios were calculated based on data collected from the pneumothorax and non-pneumothorax side separately.

Statistical analysis

SPSS 17.0 (IBM, Armonk, NY, United States) was used for statistical analysis. Normally distributed data were reported as the mean (\pm SD), and non-normally distributed data were expressed as the median (interquartile range). Comparisons between paired samples were performed using a Wilcoxon test. The receiver operating characteristic curve was constructed to evaluate the diagnostic performance of biomarkers to detect pneumothorax. The best cut-off values were defined using Youden's index. Sensitivity, specificity, positive predictive value, negative predictive value, positive likelihood ratio, negative likelihood ratio, and the corresponding 95% confidence intervals (CIs) were estimated with these cut-off values. Interobserver and intraobserver agreements were evaluated using intraclass correlation coefficients by comparing measurements made by the senior physician (RX) and resident (NZ). A *P* value < 0.05 was considered statistically significant.

RESULTS

Patient characteristics

During the study period, 61 suspected patients were admitted to our center, and a total of 45 patients were included for further analysis. The flowchart of patient selection is

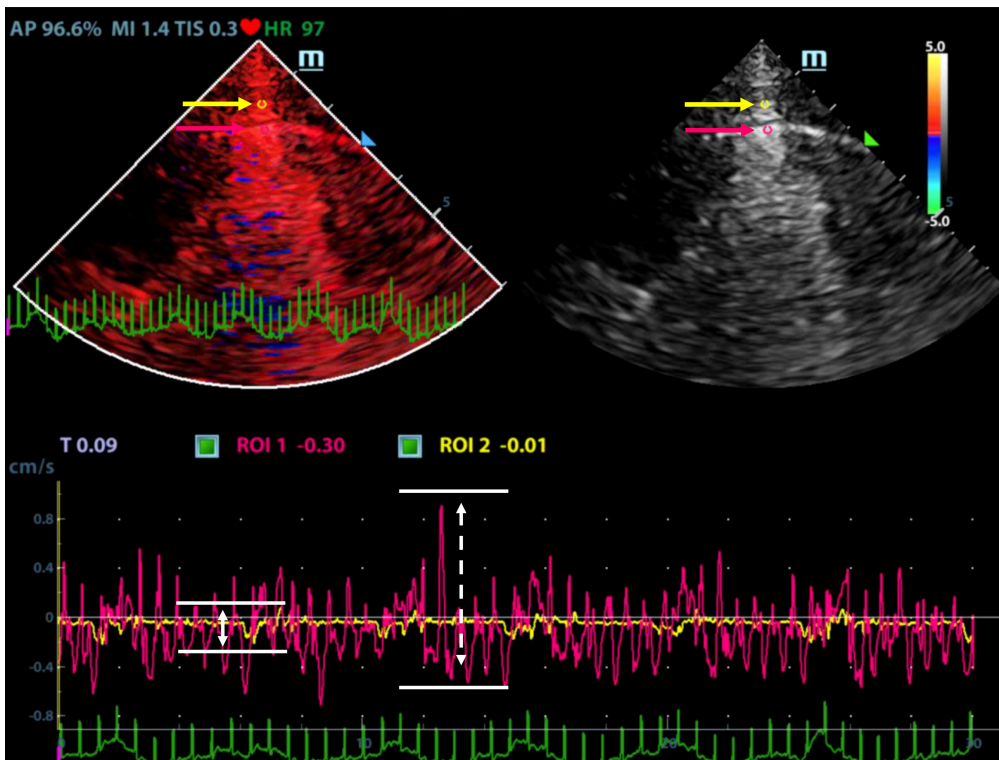


Figure 1 Peak velocity measurement. Tissue Doppler image (left), ultrasound image (right); region of interest 1 (ROI1, red dot) at the midpoint of the pleural line, ROI2 (yellow dot), 0.5 cm from the pleural line; velocity-time curve of ROI1 (red curve), velocity-time curve of ROI2 (yellow curve); velocity of ROI1 (white arrow, dotted line), peak velocity of ROI2 (white arrow, solid line).

given in **Figure 3**. Of these patients, 28 were male, and the median age was 38 years. The etiology of pneumothorax was as follows: spontaneous pneumothorax ($n = 16$) and traumatic pneumothorax ($n = 29$). Eighteen patients had pneumothorax on the left side and twenty-seven patients on the right side (**Table 1**).

Comparison between the pneumothorax and non-pneumothorax side

A total of 90 images of the included patients were obtained. Tissue Doppler features (**Figures 4 and 5** and **Videos 1-4**) are shown in **Table 2**. The CV_{max} was found to be 0.30 (0.15, 0.39) cm/s at the pneumothorax side and 0.13 (0.09, 0.19) cm/s at the non-pneumothorax side. The PS_{max} was found to be 1.62% (1.16%, 2.06%) at the pneumothorax side and 1.00% (0.71%, 1.98%) at the non-pneumothorax side. Statistical analysis showed that quantitative variables, such as the PV_{max} [0.36 (0.23, 0.41) vs 0.59 (0.38, 0.80) cm/s, $P < 0.001$], the PS_{max} [1.14 (0.41, 1.85) vs 1.90 (1.30, 3.34) %, $P = 0.001$], the PV_{max}/CV_{max} ratio [1.06 (0.85, 1.53) vs 4.93 (3.40, 7.52), $P < 0.001$], and the PS_{max}/CS_{max} ratio [0.76 (0.32, 1.05) vs 1.74 (1.30, 2.66), $P < 0.001$] of the pneumothorax side were all lower than the non-pneumothorax counterparts.

Diagnostic value of TDI measurements

The performance of TDI measurements in the diagnosis of pneumothorax are presented in **Table 3**. The results of the receiver operating characteristic analysis are shown in **Figure 6**. The areas under the receiver operating characteristic curve of the PV_{max} , PS_{max} , PV_{max}/CV_{max} and PS_{max}/CS_{max} were 0.84 (95% CI: 0.75, 0.92), 0.72 (95% CI: 0.62, 0.83), 0.99 (95% CI: 0.96, 1.00), and 0.91 (95% CI: 0.84, 0.97), respectively. For the discrimination of pneumothorax, the cut-off values of the PV_{max} , PS_{max} , PV_{max}/CV_{max} and PS_{max}/CS_{max} were calculated as 0.50 cm/s, 0.94%, 1.96, and 1.12, respectively. The corresponding sensitivities and specificities of PV_{max} , PS_{max} , PV_{max}/CV_{max} and PS_{max}/CS_{max} were 96% and 62%, 47% and 91%, 93% and 96%, and 82% and 93%, respectively.

B-Mode ultrasound

Another two physicians (one senior physician and one resident) who were blinded to the clinical diagnosis were recruited to evaluate the 90 images in B-Mode (mainly using A-line, lung sliding, lung pulse). Eighty-five episodes were correctly diagnosed by the senior physician, with the sensitivity, specificity, positive predictive value,

Table 1 Clinical characteristics of patients included in our study

Characteristics	Value
<i>n</i>	45
Male	28 (62)
Age (yr)	38 (21, 59)
Weight (kg)	63 (60, 70)
Height (cm)	16 (163, 175)
Etiology for pneumothorax	
Spontaneous pneumothorax	16 (36)
Trauma	29 (64)
Pneumothorax features	
Left	18 (40)
Right	27 (60)

Data are expressed as *n* (%) or median (interquartile range).

Table 2 Comparison of measurements obtained by tissue Doppler imaging between the pneumothorax and non-pneumothorax sides

	Pneumothorax side, <i>n</i> = 45	Non-pneumothorax side, <i>n</i> = 45	<i>P</i> value
PV _{max} (cm/s)	0.36 (0.23, 0.41)	0.59 (0.38, 0.80)	< 0.001
PS _{max} (%)	1.14 (0.41, 1.85)	1.90 (1.30, 3.34)	0.001
CV _{max} (cm/s)	0.30 (0.15, 0.39)	0.13 (0.09, 0.19)	< 0.001
CS _{max} (%)	1.62 (1.16, 2.06)	1.00 (0.71, 1.98)	0.075
PV _{max} /CV _{max}	1.06 (0.85, 1.53)	4.93 (3.40, 7.52)	< 0.001
PS _{max} /CS _{max}	0.76 (0.32, 1.05)	1.74 (1.30, 2.66)	< 0.001

Data are expressed as the median and interquartile range. PV_{max}: Peak pleural line velocity; CV_{max}: Peak chest wall tissue velocity; PS_{max}: Peak pleural line strain value; CS_{max}: Peak chest wall tissue strain value.

Table 3 The diagnostic performance of measurements obtained by tissue Doppler imaging in the diagnosis of pneumothorax

	AUC	<i>P</i> value	Cut-off value	Sensitivity	Specificity	PLR	NLR	PPV	NPV
PV _{max} (cm/s)	0.84 (0.75, 0.92)	< 0.001	0.50	96%	62%	2.53	0.07	0.72	0.93
PS _{max} (%)	0.72 (0.62, 0.83)	< 0.001	0.94	47%	91%	5.25	0.84	0.84	0.63
PV _{max} /CV _{max}	0.99 (0.96, 1.00)	< 0.001	1.96	93%	96%	21.00	0.07	0.95	0.93
PS _{max} /CS _{max}	0.91 (0.84, 0.97)	< 0.001	1.12	82%	93%	12.33	0.19	0.93	0.84

AUC: Area under receiver operating characteristic curve; PV_{max}: Peak pleural line velocity; CV_{max}: Peak chest wall tissue velocity; PS_{max}: Peak pleural line strain value; CS_{max}: Peak chest wall tissue strain value; PLR: Positive likelihood ratio; NLR: Negative likelihood ratio; PPV: Positive predictive value; NPV: Negative predictive value.

negative predictive value, and accuracy calculated as 93%, 96%, 95%, 93% and 94%, respectively. Meanwhile, eighty-four episodes were correctly diagnosed by the resident, with the sensitivity, specificity, positive predictive value, negative predictive value and accuracy calculated as 91%, 96%, 95%, 91% and 93%, respectively. Hence, it appears that the sensitivity and specificity of the TDI method are consistent with those

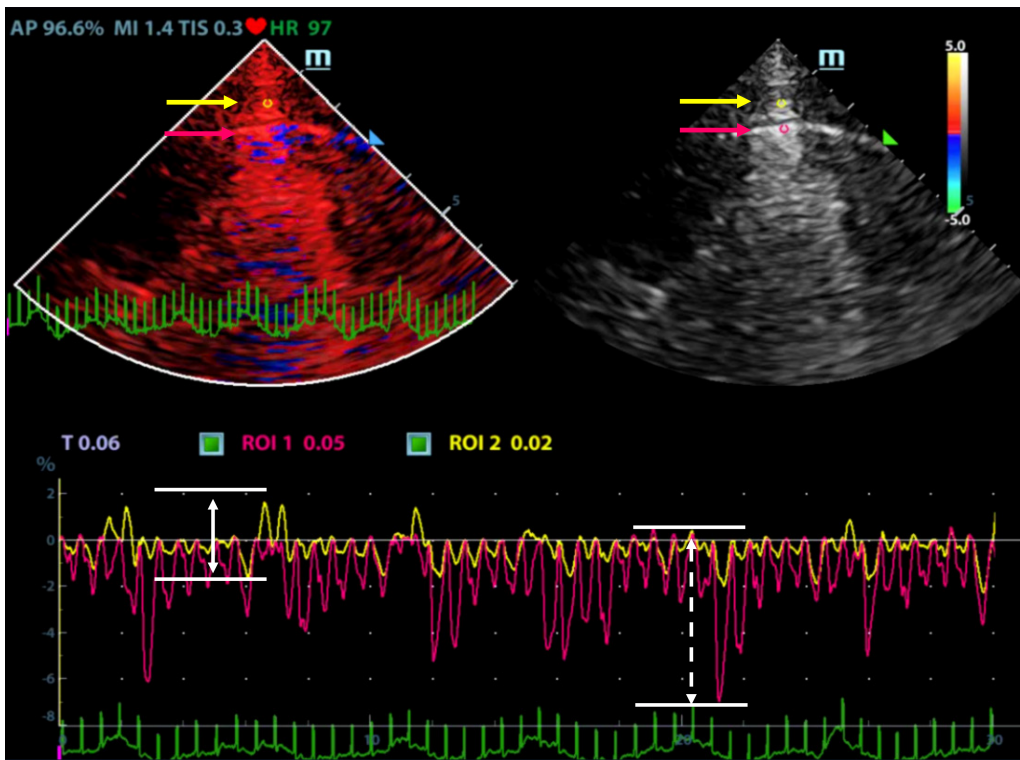


Figure 2 Peak strain measurement. Tissue Doppler image (left), ultrasound image (right); region of interest 1 (ROI1, red dot) at the midpoint of the pleural line, ROI2 (yellow dot), 0.5 cm from the pleural line; strain-time curve of ROI1 (red curve), strain-time curve of ROI2 (yellow curve); peak strain of ROI1 (white arrow, dotted line), peak strain of ROI2 (white arrow, solid line).

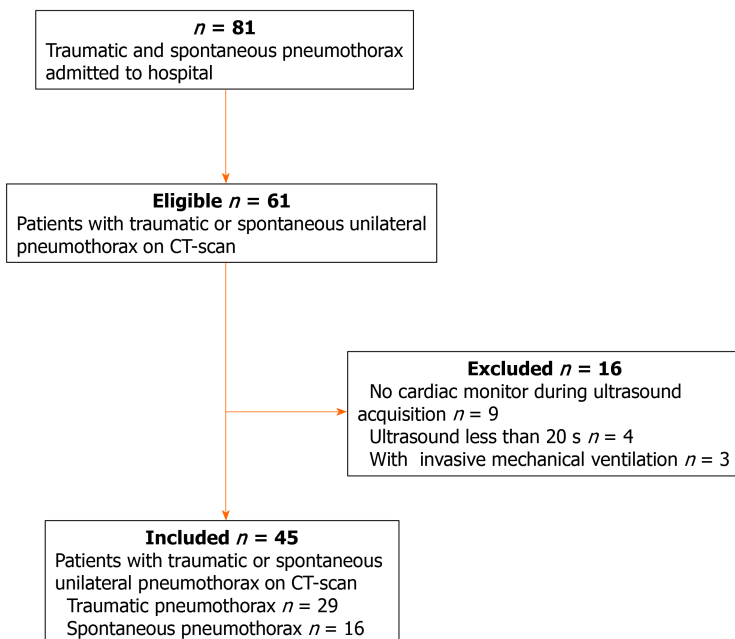


Figure 3 A flowchart of patient selection for our study. CT: Computed tomography.

of the senior physician and are better than those of the resident.

Variability of TDI measurements

The intraobserver variabilities of the PV_{max} , CV_{max} , PS_{max} and CS_{max} were 0.88 (95% CI: 0.79; 0.93), 0.82 (95% CI: 0.59; 0.92), 0.85 (95% CI: 0.75; 0.92), and 0.86 (95% CI: 0.77; 0.92), respectively (Table 4). The interobserver variabilities of the PV_{max} , CV_{max} , PS_{max} and CS_{max} were 0.79 (95% CI: 0.64; 0.88), 0.75 (95% CI: 0.48; 0.87), 0.72 (95% CI: 0.54; 0.84), and 0.75 (95% CI: 0.59; 0.86), respectively. Further analysis showed that there was no

Table 4 Variability of tissue Doppler imaging measurements

	PV _{max}	CV _{max}	PS _{max}	CS _{max}
Senior physician				
Pneumothorax	0.87 (0.78, 0.93)	0.85 (0.73, 0.91)	0.84 (0.72, 0.91)	0.88 (0.79, 0.93)
Non-pneumothorax	0.88 (0.79, 0.93)	0.82 (0.59, 0.92)	0.85 (0.75, 0.92)	0.86 (0.77, 0.92)
Resident				
Pneumothorax	0.75 (0.59, 0.87)	0.67 (0.47, 0.81)	0.64 (0.43, 0.79)	0.72 (0.48, 0.85)
Non-pneumothorax	0.79 (0.64, 0.88)	0.75 (0.48, 0.87)	0.72 (0.54, 0.84)	0.75 (0.59, 0.86)
Total				
Pneumothorax	0.77 (0.65, 0.85)	0.73 (0.60, 0.83)	0.68 (0.54, 0.80)	0.80 (0.69, 0.89)
Non-pneumothorax	0.80 (0.69, 0.87)	0.75 (0.62, 0.85)	0.76 (0.64, 0.85)	0.74 (0.62, 0.84)

PV_{max}: Peak pleural line velocity; CV_{max}: Peak chest wall tissue velocity; PS_{max}: Peak pleural line strain value; CS_{max}: Peak chest wall tissue strain value.

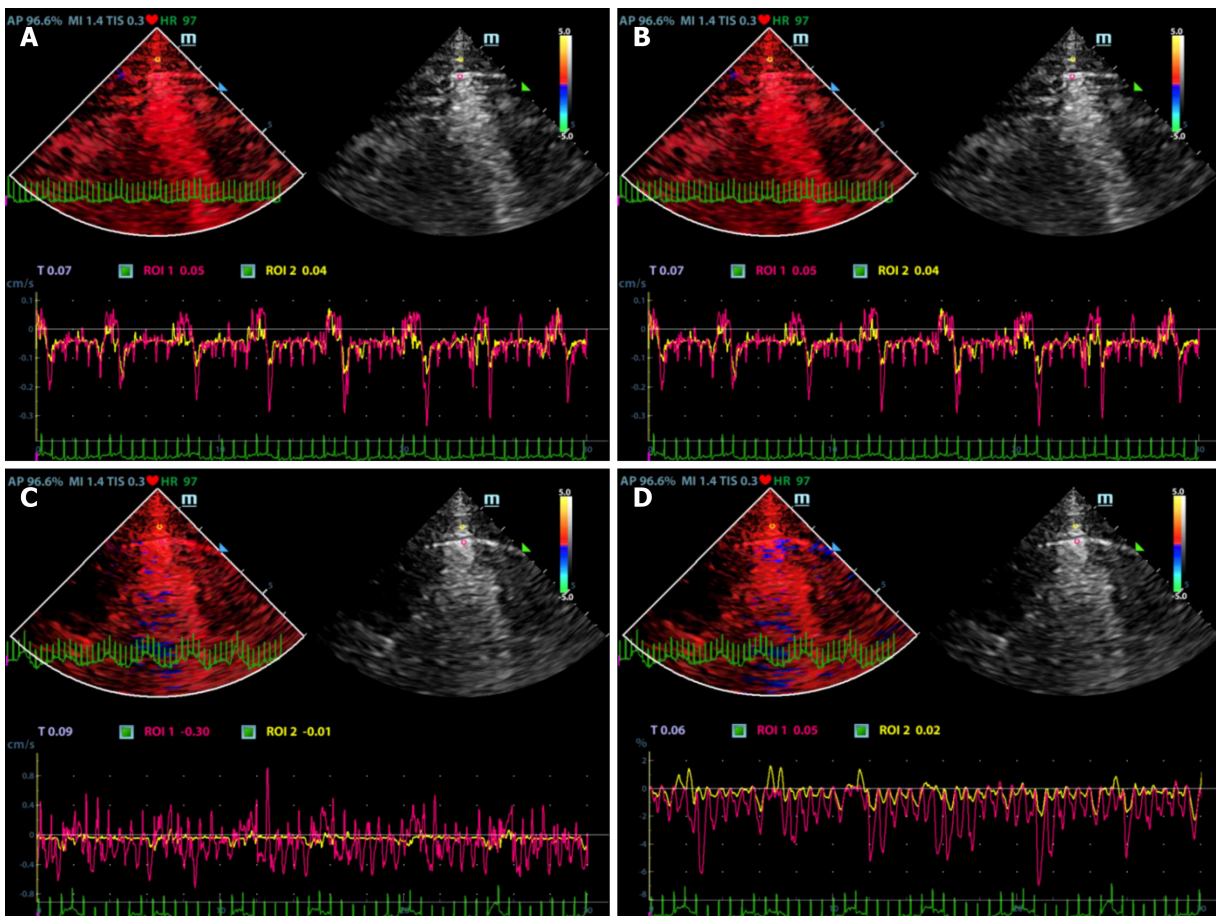


Figure 4 Tissue Doppler imaging of the pneumothorax side and the non-pneumothorax side. A: Velocity-time curve (pneumothorax side); B: Strain-time curve (pneumothorax side); C: Velocity-time curve (non-pneumothorax side); D: Strain-time curve (non-pneumothorax side).

clinically significant difference in the intraobserver variability between the two physicians (RX and NZ).

DISCUSSION

In this study, several measurements (*e.g.*, PV_{max}, CV_{max}, PS_{max}, and CS_{max}) obtained using the TDI method were evaluated for the detection of pneumothorax. Our results

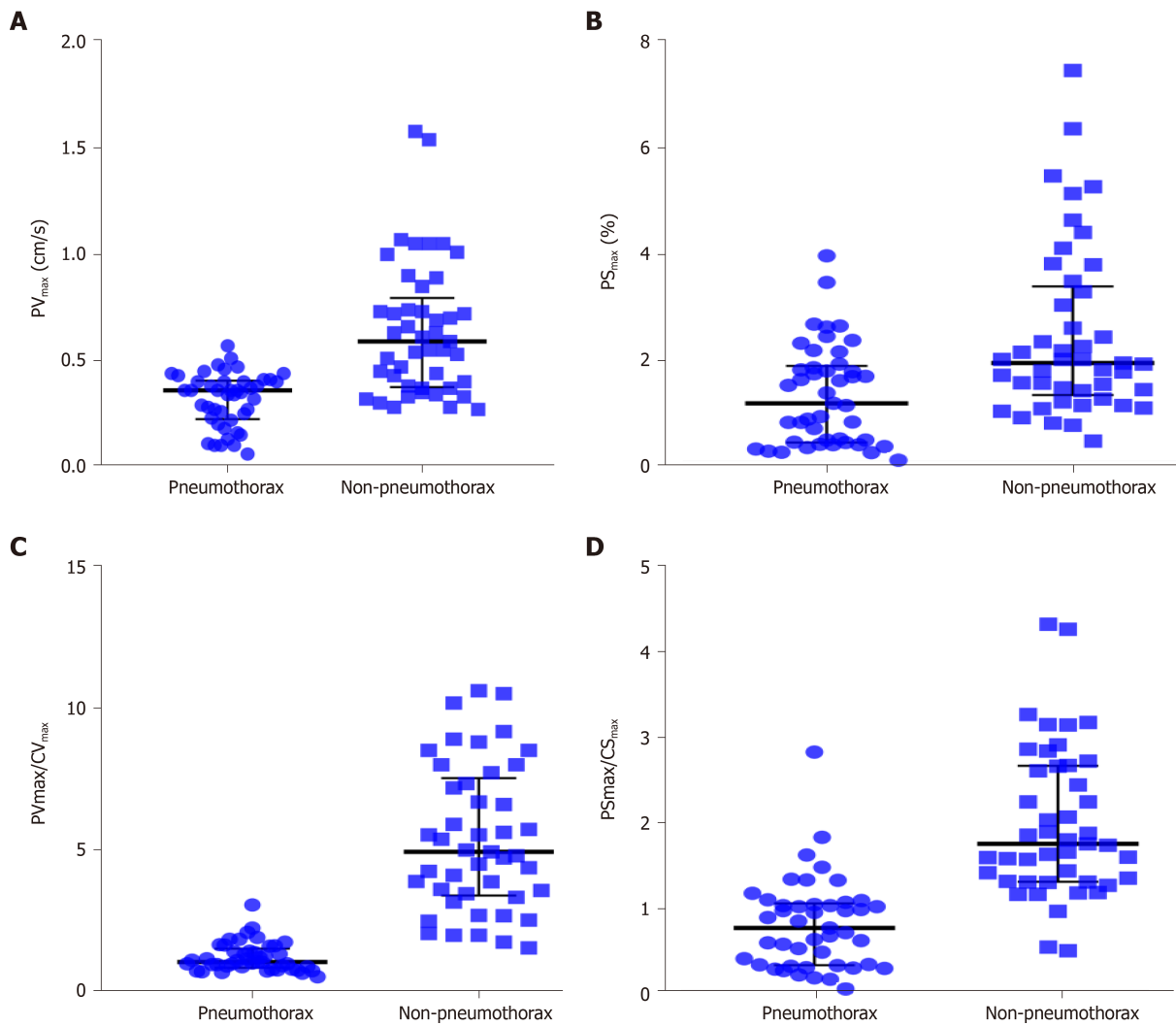


Figure 5 Scatter plot of measurements obtained by tissue Doppler imaging. A: Scatter plot of peak pleural line velocity; B: Scatter plot of peak pleural line strain value; C: Scatter plot of peak pleural line velocity/peak chest wall tissue velocity; D: Scatter plot of peak pleural line strain value/peak chest wall tissue strain value. Data are expressed as the median and interquartile range. PV_{max} : Peak pleural line velocity; CV_{max} : Peak chest wall tissue velocity; PS_{max} : Peak pleural line strain value; CS_{max} : Peak chest wall tissue strain value.

showed that compared with other indices, the PV_{max}/CV_{max} ratio exhibited the best diagnostic performance in the diagnosis of pneumothorax. Our data demonstrated that quantification analysis of pleural line movement using TDI is useful for the diagnosis of pneumothorax. To the best of our knowledge, this is the first time that measurements obtained by TDI quantification analysis of pleural line movement have been used as a diagnostic tool for pneumothorax.

The performance of lung ultrasound has been previously evaluated. However, the performance has varied widely between studies. For example, Ziapour and Haji[17] found that if the pleural movement disappears and the B-line is used, lung ultrasound exhibited a sensitivity of 78% and a specificity of 92% for pneumothorax diagnosis [17]. Press *et al*[18] found a sensitivity of 91.95% and a specificity of 89.10% for the performance of pneumothorax detection *via* lung ultrasound[18]. In addition, lung ultrasound has also been reported to exhibit low sensitivity for pneumothorax diagnosis[19]. This may be explained by the criterion of lung sliding disappearance that is often used for pneumothorax diagnosis, in which particular expertise and training is required[20]. The Mindray ultrasound device has a very useful feature by which tissue Doppler can analyze the movements of several selected arbitrary ROIs without the need to generate a heart model. Therefore, the velocity and strain of visceral and partial pleura during respiration are easy to evaluate and can be measured with pleural line movement. Hence, tissue velocity and strain imaging in the current work were innovatively used to analyze the movement of pleural movement for the pneumothorax diagnosis. In addition, our data suggest that the interobserver

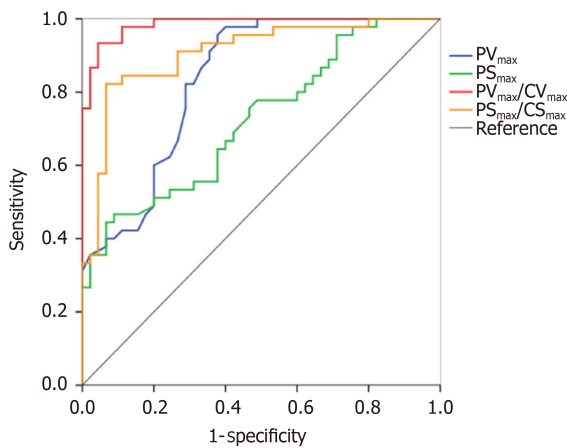


Figure 6 Receiver operating characteristic analysis of the extracted strain measurements obtained by tissue Doppler imaging. PV_{max} : Peak pleural line velocity; CV_{max} : Peak chest wall tissue velocity; PS_{max} : Peak pleural line strain value; CS_{max} : Peak chest wall tissue strain value.

variabilities of the measured indexes are moderate, and the intraobserver variabilities are low. The moderate interobserver variability is mainly due to the manual selection of ROIs. A good intraobserver agreement suggests that TDI can be well repeated by a clinical physician, indicating that this method is easy to access for the diagnosis of pneumothorax.

We found that the PV_{max}/CV_{max} calculated by data obtained from the non-pneumothorax side was greater than that from the pneumothorax side and that the PS_{max}/CS_{max} from the non-pneumothorax side was greater than that from the pneumothorax side. Compared with other indices, the PV_{max}/CV_{max} ratio exhibited the largest area under receiver operating characteristic curve for the diagnosis of pneumothorax. This suggests that the PV_{max}/CV_{max} ratio was the strongest biomarker in the diagnosis of pneumothorax in our study. In lungs under normal conditions, the velocity and strain of the pleural line seen *via* ultrasound represent the movement of the visceral pleura during respiration. By contrast, in the state of pneumothorax, the velocity and strain of the pleural line represent the movement of the parietal pleura during respiration. Therefore, when in the normal state, the velocity and strain describing the movements of the visceral and parietal pleura were higher than those in the state of pneumothorax. In addition, the pleural strain had a low sensitivity but a high specificity for pneumothorax diagnosis. This may be due to the perpendicular position of the imaging plane and that changes in the velocity of visceral pleura may be easier to find when compared with changes in the strain.

Our study also had several limitations. First, although some interesting points have been raised, the study had a small sample size. Second, most patients included in our study were thin, and our findings must be validated in obese patients as well. Third, Mindray's TDI-QA ultrasound image analysis software was used, which allows cardiac probes of the pleural line, whereas other software packages are not useful without a ventricular shape. The widespread use of this method may be limited by this shortcoming. Fourth, due to poor resolution of high-frequency probes, a phased array probe would benefit quantitative assessment of pleural line movement. Fifth, a lung ultrasound loop based on the combination of respiratory cycle and ultrasound may be more useful for the quantitative analysis of lung ultrasound[21]. Unfortunately, conventional TDI software is only applicable in echocardiography where the respiratory circle is unavailable. Therefore, the respiratory cycle may need to be introduced into the software package. Finally, a larger sample size and a prospective diagnostic study is still needed to confirm our findings.

CONCLUSION

The current study utilized TDI and quantification analysis of pleural line movement to extract several indices such as the PV_{max} , PS_{max} , CV_{max} , and CS_{max} . Our findings showed that the PV_{max} , PS_{max} , PV_{max}/CV_{max} , and PS_{max}/CS_{max} are good diagnostic biomarkers for pneumothorax. Compared with the other three biomarkers, the PV_{max}/CV_{max} ratio exhibited a better diagnostic performance. Overall, quantification analysis of pleural line movement using TDI is a useful tool for the diagnosis of pneumothorax.

ARTICLE HIGHLIGHTS

Research background

The criteria for pneumothorax using ultrasound is usually based on qualitative methodologies.

Research motivation

Tissue Doppler imaging (TDI) technology might discriminate pneumothorax by quantifying pleural line movement. Based on that, pneumothorax might be diagnosed in an objective way.

Research objectives

TDI can quantify pleural line movement while diagnosing pneumothorax.

Research methods

Forty-five patients with unilateral pneumothorax were recruited. The pneumothorax side and contralateral normal lung side were then compared using several indices extracted from TDI, such as peak pleural line velocity (PVmax), peak chest wall tissue velocity (CVmax), peak pleural line strain value (PSmax), peak chest wall tissue strain value, PVmax/CVmax, and PSmax/peak chest wall tissue strain value. Receiver operating characteristic analysis was used to evaluate the performance of these quantitative assessments for pneumothorax diagnosis.

Research results

PVmax, PSmax, PVmax/CVmax, PSmax/peak chest wall tissue strain value obtained on the pneumothorax side were lower than those on the non-pneumothorax side. The PVmax/CVmax was the best index for the detection of pneumothorax with an area under receiver operating characteristic curve of 0.99.

Research conclusions

Therefore, we concluded that TDI is an effective tool for the diagnosis of pneumothorax.

Research perspectives

Further research is required to validate our findings in suspected cases.

REFERENCES

- 1 Kelly AM, Weldon D, Tsang AY, Graham CA. Comparison between two methods for estimating pneumothorax size from chest X-rays. *Respir Med* 2006; **100**: 1356-1359 [PMID: 16406560 DOI: 10.1016/j.rmed.2005.11.022]
- 2 Beckmann U, Gillies DM, Berenholtz SM, Wu AW, Pronovost P. Incidents relating to the intra-hospital transfer of critically ill patients. An analysis of the reports submitted to the Australian Incident Monitoring Study in Intensive Care. *Intensive Care Med* 2004; **30**: 1579-1585 [PMID: 14991102 DOI: 10.1007/s00134-004-2177-9]
- 3 Kirkpatrick AW, Sirois M, Laupland KB, Liu D, Rowan K, Ball CG, Hameed SM, Brown R, Simons R, Dulchavsky SA, Hamilton DR, Nicolaou S. Hand-held thoracic sonography for detecting post-traumatic pneumothoraces: the Extended Focused Assessment with Sonography for Trauma (EFAST). *J Trauma* 2004; **57**: 288-295 [PMID: 15345974 DOI: 10.1097/01.ta.0000133565.88871.e4]
- 4 Xirouchaki N, Magkanas E, Vaporidi K, Kondili E, Plataki M, Patrianakos A, Akoumianaki E, Georgopoulos D. Lung ultrasound in critically ill patients: comparison with bedside chest radiography. *Intensive Care Med* 2011; **37**: 1488-1493 [PMID: 21809107 DOI: 10.1007/s00134-011-2317-y]
- 5 Lichtenstein DA, Menu Y. A bedside ultrasound sign ruling out pneumothorax in the critically ill. Lung sliding. *Chest* 1995; **108**: 1345-1348 [PMID: 7587439 DOI: 10.1378/chest.108.5.1345]
- 6 Lichtenstein D, Mezière G, Biderman P, Gepner A. The "lung point": an ultrasound sign specific to pneumothorax. *Intensive Care Med* 2000; **26**: 1434-1440 [PMID: 11126253 DOI: 10.1007/s001340000627]
- 7 Moreno-Aguilar G, Lichtenstein D. Lung ultrasound in the critically ill (LUCI) and the lung point: a sign specific to pneumothorax which cannot be mimicked. *Crit Care* 2015; **19**: 311 [PMID: 26345706 DOI: 10.1186/s13054-015-1030-6]
- 8 Lichtenstein DA, Mezière GA. Relevance of lung ultrasound in the diagnosis of acute respiratory failure: the BLUE protocol. *Chest* 2008; **134**: 117-125 [PMID: 18403664 DOI: 10.1378/chest.07-2800]

- 9 **Del Colle A**, Carpagnano GE, Feragalli B, Foschino Barbaro MP, Lacedonia D, Scioscia G, Quarato CMI, Buonamico E, Tinti MG, Rea G, Cipriani C, Frongillo E, De Cosmo S, Guglielmi G, Sperandeo M. Transthoracic ultrasound sign in severe asthmatic patients: a lack of "gliding sign" mimic pneumothorax. *BJR Case Rep* 2019; **5**: 20190030 [PMID: 31938562 DOI: 10.1259/bjrcr.20190030]
- 10 **Gelabert C**, Nelson M. Bleb point: mimicker of pneumothorax in bullous lung disease. *West J Emerg Med* 2015; **16**: 447-449 [PMID: 25987927 DOI: 10.5811/westjem.2015.3.24809]
- 11 **Slater A**, Goodwin M, Anderson KE, Gleeson FV. COPD can mimic the appearance of pneumothorax on thoracic ultrasound. *Chest* 2006; **129**: 545-550 [PMID: 16537850 DOI: 10.1378/chest.129.3.545]
- 12 **Ding W**, Shen Y, Yang J, He X, Zhang M. Diagnosis of pneumothorax by radiography and ultrasonography: a meta-analysis. *Chest* 2011; **140**: 859-866 [PMID: 21546439 DOI: 10.1378/chest.10-2946]
- 13 **Schrift D**, Barron K, Wagner M, Arya R. A case report of lung ultrasound missing a pneumothorax due to patient positioning. *Ultrasound* 2017; **25**: 248-250 [PMID: 29163662 DOI: 10.1177/1742271X17708473]
- 14 **Mullens W**, Borowski AG, Curtin RJ, Thomas JD, Tang WH. Tissue Doppler imaging in the estimation of intracardiac filling pressure in decompensated patients with advanced systolic heart failure. *Circulation* 2009; **119**: 62-70 [PMID: 19075104 DOI: 10.1161/CIRCULATIONAHA.108.779223]
- 15 **Hoffmann S**, Mogelvang R, Sogaard P, Iversen AZ, Hvelplund A, Schaadt BK, Fritz-Hansen T, Galatius S, Risum N, Biering-Sørensen T, Jensen JS. Tissue Doppler echocardiography reveals impaired cardiac function in patients with reversible ischaemia. *Eur J Echocardiogr* 2011; **12**: 628-634 [PMID: 21757478 DOI: 10.1093/ejehoccard/er094]
- 16 **Yu CM**, Goresan J 3rd, Bleeker GB, Zhang Q, Schalij MJ, Suffoletto MS, Fung JW, Schwartzman D, Chan YS, Tanabe M, Bax JJ. Usefulness of tissue Doppler velocity and strain dyssynchrony for predicting left ventricular reverse remodeling response after cardiac resynchronization therapy. *Am J Cardiol* 2007; **100**: 1263-1270 [PMID: 17920368 DOI: 10.1016/j.amjcard.2007.05.060]
- 17 **Ziapour B**, Haji HS. "Anterior convergent" chest probing in rapid ultrasound transducer positioning vs formal chest ultrasonography to detect pneumothorax during the primary survey of hospital trauma patients: a diagnostic accuracy study. *J Trauma Manag Outcomes* 2015; **9**: 9 [PMID: 26697105 DOI: 10.1186/s13032-015-0030-5]
- 18 **Press GM**, Miller SK, Hassan IA, Alade KH, Camp E, Junco DD, Holcomb JB. Prospective evaluation of prehospital trauma ultrasound during aeromedical transport. *J Emerg Med* 2014; **47**: 638-645 [PMID: 25281177 DOI: 10.1016/j.jemermed.2014.07.056]
- 19 **Trovato G**, Sperandeo M. Lung Ultrasound in Pneumothorax: The Continuing Need for Radiology. *J Emerg Med* 2016; **51**: 189-191 [PMID: 27317611 DOI: 10.1016/j.jemermed.2015.01.045]
- 20 **Alrajab S**, Youssef AM, Akkus NI, Caldito G. Pleural ultrasonography vs chest radiography for the diagnosis of pneumothorax: review of the literature and meta-analysis. *Crit Care* 2013; **17**: R208 [PMID: 24060427 DOI: 10.1186/cc13016]
- 21 **Duclos G**, Bobbia X, Markarian T, Muller L, Cheyssac C, Castillon S, Resseguier N, Boussuges A, Volpicelli G, Leone M, Zieleskiewicz L. Speckle tracking quantification of lung sliding for the diagnosis of pneumothorax: a multicentric observational study. *Intensive Care Med* 2019; **45**: 1212-1218 [PMID: 31359081 DOI: 10.1007/s00134-019-05710-1]



Published by **Baishideng Publishing Group Inc**
7041 Koll Center Parkway, Suite 160, Pleasanton, CA 94566, USA

Telephone: +1-925-3991568

E-mail: bpgoffice@wjgnet.com

Help Desk: <https://www.f6publishing.com/helpdesk>

<https://www.wjgnet.com>

